Anal. Chem. **2004,** *76,* 4395−4405

Transport Model of Chemical Secretion Process for Tracking Exocytotic Event Dynamics Using Electroanalysis

Tai-Hsi Fan and Andrei G. Fedorov*

Multiscale Integrated Thermofluidics Laboratory, G. W. Woodruff School of Mechanical Engineering, Georgia Institute of Technology, Atlanta, Georgia 30332-0405

A unified model is developed to analyze the key features of the chemical secretion process observed in experimental studies of various vesicles with application to electroanalytical measurements of vesicular exocytosis. The intimately coupled dynamics and kinetics are simultaneously resolved based on continuum fluid flow, mass transport, and linear elasticity theories combined with biomembrane mechanics. We report three case studies of exocytosis, including a large electroporated granule of the mast cell, a small and clear synaptic vesicle, and a medium size vesicle in the chromaffin cell. The simulation results for each case are compared with electroanalytical measurements from the literature. The results provide a theoretical ground for defining the rate-controlling step(s) of an exocytotic sequence, allowing interpretation of electroanalysis data. Thus, it provides a tool for theoretical verification of competing hypotheses of what controls/limits messenger release during exocytosis. Simulations show that the pore size, the pore opening velocity, and the swelling dynamics of the granule matrix play the key roles in controlling the messenger release kinetics.

Vesicular exocytosis is a process by which a vesicle within a cell fuses to a plasma membrane and releases its contents, one or several biochemical agents, into an extracellular medium. This process is an important mechanism that defines cell signaling and intercellular communication. For example, an abnormal regulation of the secretion process may cause many human diseases in nervous and endocrine systems. A simplified description of the exocytotic event starts with protein synthesis and vesicle packing in the cell cytoplasm, followed by the vesicle transport within the cell, fusion of the vesicle to the cell membrane by a working protein, and ends with the release of the vesicle content, that is one or several chemical messengers included in the vesicle granule matrix, to the extracellular medium. In the release process, several fundamental issues have been a focus of active research for more than a decade. These include the signal pathway that leads to membrane fusion, the structure and conformation change of the working proteins that mediate the pore opening, the expansion of a small fusion pore followed by the membrane unfolding, the role of the swelling granule, the signals that trigger or inhibit the overall secretion process, and transport of these chemical messengers in a cellular environment. It is too ambitious and perhaps even unrealistic to expect that a general theory can be developed for such a complex biophysical process as exocytosis. In this paper we only focus on the vesicle postfusion step of the exocytotic sequence, aiming for development of a theoretically sound modeling framework that can be used to interpret the electroanalytical measurements of exocytosis.

The transport phenomena of a dynamic exocytotic event involve fluid (due to intra- and extracellular physiological liquid environment) and solid (due to membrane tension/compression and granule swelling) mechanics that either promote or resist the messenger release from the fused vesicle through a fusion pore and a thin cleft to the binding zone of a specific target cell. Once the fusion pore is opened, the fused membrane continues unfolding until its minimum energy state is achieved. Both the cytoskeleton network that supports the plasma membrane of the host cell and the prestressed vesicle membrane provide the tension force to drive the event dynamics. The fused membrane may have nonhomogeneous tension and perhaps even locally varying elastic properties that, together with the expansion of the swelling granule matrix and the viscous drag forces in the fluid inside and outside of the cell, drive expansion of the fusion pore and control/limit the messenger release. The granule matrix inside the vesicle is a polyelectrolyte mixture, part of which is a network of proteins, effectively cross-linked by divalent cations such as Ca^{2+}, and the rest of the interstice consists of highly concentrated secretion messengers and other ionic species. Once granule swelling is triggered by biochemical changes in the extracellular environment, the matrix transitions to a fully swollen state, and the negatively charged protein network either dissolves in the environment or resists further elastic expansion by stretching the polymer strands to maintain its structure. Similar to an ion exchanger, this transition phenomenon has a cascade behavior triggered by monovalent cations such as Na^+ and K^+.[1,2] These ions from the solution medium replace the divalent polymer cross-

* To whom correspondence should be addressed. E-mail: andrei.fedorov@me.gatech.edu.

(1) Marszalek, P. E.; Farrell, B.; Verdugo, P.; Fernandez, J. M. *Biophys. J.* **1997**, *73*, 1169−1183.
(2) Kennedy, R. T.; Huang, L.; Atkinson, M. A.; Dush, P. *Anal. Chem.* **1993**, *65*, 1882−1887.

10.1021/ac049748g CCC: $27.50
Published on Web 07/02/2004

linkers and maintain electroneutrality. While the molecular messengers and cross-linkers are released from the interstice of the protein network, water molecules gradually fill in the space. These phenomena are well-known in synthetic polymer systems,[3] but it has not been clearly established how they can be coupled to other transport processes involved in an exocytotic event sequence.

Many key features involved in the postfusion event of exocytosis have been observed by chronoamperometric monitoring using microelectrode-based biosensors,[1,4−12] but the intimately coupled dynamics and the messenger transport processes have yet to be clearly established. Perhaps owing to the lack of detailed biochemical information, a broad range of the characteristic length and time scales, and an overwhelming complexity of the phenomena, there have been only a few theoretical models developed, all of which are limited to a semiempirical diffusion-like transport and a simplified cell/vesicle geometry. Stiles et al.[13] used Monte Carlo simulations to predict the passive diffusion behavior of acetylcholine from a small and clear synaptic vesicle with spatial and temporal resolutions of tenths of nanometers and microseconds, respectively. Amatore's and Wightman's groups[10,11] developed a semiempirical diffusion−kinetics model to separate the effect of the pore opening kinetics and diffusional transport based on their experimental observations of adrenaline release from chromaffin cells. Recently, Farrell and Cox[14] also developed a diffusion model for a class of pore opening functions as a dynamic boundary condition to reproduce the efflux that matches experiments with mast cells for various vesicle sizes.

In this paper, we assume that initially the fusion pore is in an opened state and the fused membrane has a homogeneous simple bilayer structure. The presence of cytoskeleton is not directly modeled, but it can be potentially included through the parameters in the macroscopic tension, bending, and viscous forces that govern unfolding of the membrane. We assume that both the extracellular environment and the intracellular fluids are homogeneous, incompressible Newtonian fluids with the same densities but with different viscosities. The membrane is mathematically treated as an infinitesimally thin and perfectly smooth interface separating intra- and extracellular environments. We neglect molecular level interactions, all short-range effects, thermally induced membrane fluctuations, and any heat generation due to nonequilibrium, rapid matrix swelling. In this idealized system,

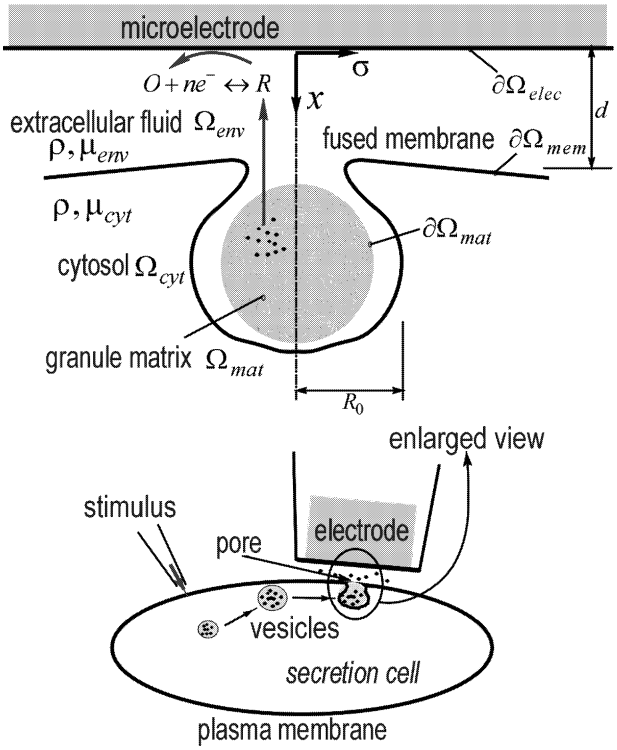

Figure 1. Schematic of electroanalytical monitoring of exocytosis using a microelectrode (bottom) and an idealized simulation domain (top).

we further assume that the mechanical work performed by the swelling granule matrix on the vesicle membrane can be neglected in the limit of small deformations. The set of models developed are based on continuum theories with the length and time scales relevant to three specific experimental studies of exocytosis. These models are governed by the following: (i) the quasi-steady Stokes equations of fluid motion induced by unfolding of the membrane, (ii) a transient, nonhomogeneous diffusion equation for the molecular messenger distribution inside of the swelling granule matrix, and (iii) a diffusion−advection equation for the transport of these chemical messengers in the extracellular medium. We apply Helfrich's curvature energy theory[15] and Zhong-can's equilibrium membrane equation,[16] augmented by the constraint equation for local membrane incompressibility, as a quasi-steady, nonlinear moving boundary condition to link the fluid stress fields on both sides of the fused membrane. In addition, we apply the Tanaka, Hocker, and Benedek (THB)[17,18] hydrogel model to predict the swelling behavior of the protein network in the granule matrix.

SCALING OF THE PHENOMENA

Figure 1 shows an axisymmetric schematic of the idealized physical arrangement used for model development. It includes the intracellular cytosol (Ω_{cyt}), the extracellular fluid environment (Ω_{env}), and a separating boundary established by a fused vesicle/

(3) Helfferich, F. *Ion Exchange*; Dover Publications: New York, 1995.
(4) Schroeder, T. J.; Jankowski, J. A.; Kawagoe, K. T.; Wightman, R. M.; Lefrou, C.; Amatore, C. *Anal. Chem.* **1992**, *64*, 3077−3083.
(5) Alvarez de Toledo, G.; Fernandez-Chacon, R.; Fernandez, J. M. *Nature* **1993**, *363*, 554−557.
(6) Bruns, D.; Jahn, R. *Nature* **1995**, *377*, 62−65.
(7) Stiles, J. R.; Helden, D. V.; Bartol, T. M.; Salpeter, E. E.; Salpeter, M. M. *Proc. Natl. Acad. Sci. U.S.A.* **1996**, *93*, 5747−5752.
(8) Marszalek, P. E.; Farrell, B.; Verdugo, P.; Fernandez, J. M. *Biophys. J.* **1997**, *73*, 1160−1168.
(9) Travis, E. R.; Wightman R. M. *Annu. Rev. Biophys. Biomol. Struct.* **1998**, *27*, 77−103.
(10) Amatore, C.; Bouret, Y.; Midrier, L. *Chem. Eur. J.* **1999**, *5*, 2151−2162.
(11) Amatore, C.; Bouret, Y.; Travis, E. R.; Wightman, R. M. *Biochimie* **2000**, *82*, 481−496.
(12) Troyer, K. P.; Heien, M. L. A. V.; Venton, B. J.; Wightman R. M. *Curr. Opin. Chem. Biol.* **2002**, *6*, 696−703.
(13) Stiles, J. R.; Helden, D. V.; Bartol, T. M.; Salpeter, E. E.; Salpeter, M. M. *Proc. Natl. Acad. Sci. U.S.A.* **1996**, *93*, 5747−5752.
(14) Farrell, B.; Cox, S. *Bull. Math. Biol.* **2002**, *64*, 979−1010.
(15) Helfrich, W. *Z. Naturforsch., C* **1973**, *28*, 693.
(16) Zhong-can, O.-Y.; Helfrich, W. *Phys. Rev. A* **1989**, *39*, 5280−5288.
(17) Tanaka, T.; Hocker, L. O.; Benedek, G. B. *J. Chem. Phys.* **1973**, *59*, 5151−5159.
(18) Tanaka, T.; Fillmore, D. J. *J. Chem. Phys.* **1979**, *70*, 1214−1218.

plasma membrane ($\partial\Omega_{mem}$). The domain of a granule matrix (Ω_{mat}) is bounded by an interface ($\partial\Omega_{mat}$), and the surface of the microelectrode ($\partial\Omega_{elec}$) is placed adjacent to the pore in the extracellular environment. An axisymmetric three-dimensional hourglass shape[19] is employed as an initial configuration with the fusion pore and granule matrix positioned along the centerline. The model input parameters include the initial radius of a secretion vesicle, R_0, the experimentally observed maximum expansion velocity of the fusion pore, V_0, and a fixed electrode-to-membrane separation distance, d ($d \sim R_0$). The extracellular fluid is characterized by density ρ and dynamic viscosity μ_{env}. The cytosol is approximated by the same fluid density, but has a different viscosity μ_{cyt}. The simplified bilayer structure of the fused membrane is characterized by its intrinsic elastic properties such as an effective bending rigidity and local tension/compression force γ. The electrochemical reaction at the microelectrode surface is mathematically treated as an instantaneous event.

By assuming that the exocytosis dynamics is driven by the interplay between the membrane relaxation (unfolding) and release of molecular messengers from the vesicle granule, six time scales can be identified as relevant to the problem in hand and expressed in terms of the length scale $l \sim R_0$ as follows: (i) the fusion pore expansion time scale, $t_{pore} \sim R_0/V_0$, characterizes the pore expansion dynamics, (ii) the fluid viscous diffusion time scale, $t_{visc} \sim \rho R_0^2/\mu_{cyt}$, characterizes the viscous driving force of fluid motion, (iii) the messenger diffusion time scale in the bulk electrolyte, $t_{diff,bulk} \sim R_0^2/D_{bulk}$, characterizes the molecular transport to the electrode surface through the extracellular electrolyte solution, (iv) the messenger diffusion time scale in the granule matrix, $t_{diff,matrix} \sim R_0^2/D_{matrix}$, characterizes the apparent diffusion behavior through the protein network inside the granule matrix, (v) the collective diffusion time scale of the swelling matrix $t_{diff,swell} \sim R_0^2/D_{swell}$, controls the linear swelling dynamics of the protein matrix, and (vi) the electron transfer time scale of the irreversible oxidation reaction at the electrode−solution interface, $t_{reaction}$, is assumed to be much faster than all dynamics presented. Note that D_{bulk} and D_{matrix} are the corresponding messenger diffusivities in the bulk electrolyte and in the protein matrix. The physical meaning of the collective swelling diffusivity D_{swell} is discussed in the Mathematical Model.

We apply the model to three cases for which sufficiently detailed experimental data exist: (a) the large size vesicles in mast cells $R_0 \sim 2.5\ \mu$m,[1,8] with a pore expansion velocity $V_0 \sim 20\ \mu$m/s;[14] (b) the small clear synaptic vesicles, $R_0 \sim 20$ nm, with a pore expansion velocity $V_0 \sim 25\ \mu$m/s;[6,7] (c) the medium size vesicles of the chromaffin cells $R_0 \sim 150$ nm[11] with the pore expansion velocity V_0 ranging between 0.37 μm/s (beginning of the process) and 18 μm/s (end of process),[11] wherein the slow and fast opening velocities are deduced from the capacitance data measured by the vesicle membrane area incorporated into the cell membrane. Given $\rho \sim 10^3$ kg/m^3, $\mu_{cyt} \geq \mu_{env} \sim 1.5 \times 10^{-3}$ kg/m·s (1.5 cp), $D_{bulk} \sim 6.0 \times 10^{-10}$ m^2/s,[1,13] $D_{matrix} \sim 2.0 \times 10^{-12}$ m^2/s,[1] and $D_{swell} \sim 1.4 \times 10^{-11}$ m^2/s,[1] the characteristic time scales for three case studies can be approximated

$$t_{pore} \sim \text{(a) } 0.125 \text{ s, (b) } 8.0 \times 10^{-4} \text{ s, and (c) } 8.33 \times 10^{-3} \text{ s} \quad (1)$$

$$t_{visc} \sim \text{(a) } 4.2 \times 10^{-6} \text{ s, (b) } 2.7 \times 10^{-10} \text{ s, and (c) } 1.5 \times 10^{-8} \text{ s}$$

$$t_{diff,bulk} \sim \text{(a) } 1.0 \times 10^{-2} \text{ s, (b) } 6.7 \times 10^{-7} \text{ s, and (c) } 3.75 \times 10^{-5} \text{ s}$$

$$t_{diff,matrix} \sim \text{(a) } 3.1 \text{ s, (b) no granule matrix, and (c) } 1.13 \times 10^{-2} \text{ s}$$

$$t_{diff,swell} \sim \text{(a) } 0.45 \text{ s, (b) no granule matrix, and (c) } 1.6 \times 10^{-3} \text{ s}$$

These time scales can be grouped into the following categories based on their relative order of magnitudes

$$\left.\begin{array}{l}\text{(a)} t_{diff,matrix} > t_{diff,swell} \sim t_{pore} \\ \text{(b)} t_{pore} \\ \text{(c)} t_{diff,matrix} \sim t_{pore} > t_{diff,swell}\end{array}\right\} > t_{diff,bulk} \gg t_{visc},\ t_{reaction} \quad (2)$$

Equation 2 establishes a generality in the dynamics of the exocytotic event regardless of the specific vesicle type and allows us to reduce the complexity of the analysis. First, the oxidation reactions at the electrode/electrolyte interface are very fast and can be treated as equilibrium surface phenomena. Second, the extremely small viscous diffusion time scale suggests the quasi-steady approach to the analysis of the fluid motion, and similarly, the quasi-steady stress balance equation for the deforming membrane. Third, scaling suggests that a transient analysis of the swelling dynamics of the granule matrix is required for cases a and c because the messenger concentration field inside the vesicle matrix is first dominated by the swelling behavior on a shorter time scale, $t_{diff,swell}$, and later by the matrix diffusion on a longer time scale, $t_{diff,matrix}$. The close proximity of the matrix swelling and matrix diffusion time scales makes these two dynamic processes intimately coupled, thus requiring simultaneous resolution. In addition to direct observation of the time scales, three dimensionless groups can also be used to justify the simplified system: first the ratio of $t_{diff,bulk}$ to t_{pore} generates the Peclet number, which compares the species transport by advection and bulk diffusion effects

$$Pe_{fluid} = \frac{t_{diff,bulk}}{t_{pore}} = \frac{V_0 R_0}{D_{bulk}} \sim \text{(a) } 8.3 \times 10^{-2}, \text{ (b) } 8.4 \times 10^{-4}, \text{ and (c) } 4.5 \times 10^{-3} \quad (3)$$

A very small Peclet number in case b suggests that the advection effect induced by membrane relaxation is negligible. Physically it implies that the pore expansion is relatively slow on the time scale of $t_{diff,bulk}$. In cases a and c, the bulk advection effects are small but may not be negligible. Second, the comparison of bulk

(19) Chandler, D. E.; Heuser, J. E. *J. Cell Biol.* **1980**, *86*, 666−674.

and matrix diffusion times scales, $t_{diff,bulk}$ versus $t_{diff,matrix}$, generates the diffusivity ratio

$$\frac{t_{diff,bulk}}{t_{diff,matrix}} = \frac{D_{matrix}}{D_{bulk}} \sim \text{(a) } 3.33 \times 10^{-3}\text{, (b) no granule, and (c) } 3.33 \times 10^{-3} \quad (4)$$

The small values imply that the dynamics of the process in cases a and c is limited by the diffusion in the vesicle granule matrix. Thus, if time scale $t_{diff,matrix}$ needs to be resolved, the quasi-steady analysis can be used for the transport phenomena in the liquid environment, whereas a transient diffusion system should be applied to the matrix domain. Third, owing to the very low Reynolds number, $Re = \rho V_0 R_0/\mu_{cyt}$, from 3.3×10^{-7} to 3.3×10^{-5}, the flow inertial forces are negligibly small as compared to the viscous forces, and thus, the nonlinear advection terms in the Navier−Stokes equations can be dropped.

We also neglect the electroosmotic effect because the bulk ionic strength of the solution under normal physiological conditions is relatively strong. That is, if the buffer has an ionic strength of 0.15 M then the corresponding Debye length is 0.78 nm and the ionic migration time scale[20] is of the order of 10 ps at room temperature. This time scale is many orders of magnitude smaller than the characteristic time scales relevant to electroanalysis reported in our case studies. This indicates that the local electrochemical equilibrium prevails and the concentration of the ionic species obeys the Boltzmann distribution. Further, since the electrical double layer is confined to very thin regions (<1 nm) near the membrane and electrode surfaces, the electric field outside this regions (in the bulk) is essentially fully screened, and therefore, one can neglect the Coulombic forces acting on the electrolyte.

MATHEMATICAL MODEL

An axisymmetric coordinate system with the origin affixed to the electrode surface and the axial coordinate axis x pointed downward (Figure 1) is used to simulate (i) the intracellular and extracellular fluid motion, messenger transport, and the membrane deformation, and (ii) the granule elastic deformation and intramatrix molecular messenger transport. Due to the lack of detailed biological information about extrusion behavior of the granule matrix, we assume that the matrix is suspended at a fixed position in the extracellular fluid that fills the vesicle when the pore is opened. The messenger transport in the fluid as well as in the granule matrix is governed by the general transient, nonhomogeneous transport equation

$$\frac{\partial C(\mathbf{x})}{\partial t} + \nabla\cdot(C(\mathbf{x})\mathbf{v}(\mathbf{x})) = D\nabla^2 C(\mathbf{x}) + S(\mathbf{x}), \quad \mathbf{x} \in \Omega \quad (5)$$

where C is the local neurotransmitter concentration, S is the sink/source term due to homogeneous chemical reactions involving neurotransmitters (if present), $\mathbf{v}$ is the bulk advection fluid velocity vector, and D is a diffusivity (assumed constant). To make the presentation of the model development clear, we first introduce the model for the fluid motion as it remains the same for all three cases a, b, and c considered here. Then, we discuss on the case-by-case basis the models governing messenger transport for cases a, b, and c, because of the difference in the time scales leading to differences in the mathematical formulation. Finally, the fluid and mass transport models are coupled by the initial and boundary conditions, which are also of a general nature and equally applicable to all three cases a, b, and c. Such a presentation order not only makes the mathematical logic clearer, but also allows for the case-by-case comparison of the model predictions with the experimental results from the literature.

The Fluid System. According to the scaling arguments presented in the previous section, the dynamics of both fluids, i.e., inside (Ω_{cyt}) and outside (Ω_{env}) of the cell (Figure 1), is governed by the quasi-steady Stokes equation and the continuity equation:

$$-\nabla p(\mathbf{x}) + \mu_{env}\nabla^2\mathbf{v}(\mathbf{x}) = 0, \quad \nabla\cdot\mathbf{v}(\mathbf{x}) = 0 \qquad \text{for } \mathbf{x} \in \Omega_{env} \quad (6a)$$

$$-\nabla p(\mathbf{x}) + \mu_{cyt}\nabla^2\mathbf{v}(\mathbf{x}) = 0, \quad \nabla\cdot\mathbf{v}(\mathbf{x}) = 0 \qquad \text{for } \mathbf{x} \in \Omega_{cyt} \quad (6b)$$

where p, $\mathbf{v}$, μ_{env}, μ_{cyt} are the pressure, the velocity vector, and the dynamic viscosities of the extracellular environment and cytosol, respectively, and $\mathbf{x}$ denotes a position vector in the Cartesian coordinate system. For both eqs 6a and 6b, the hydrodynamic pressure is scaled by the fluid viscous force based on the cytosol viscosity μ_{cyt}, so that the dimensionless Stokes equations can be written as, regardless of the time scale selected,

$$-\nabla p + \lambda\nabla^2\mathbf{v} = 0, \quad \nabla\cdot\mathbf{v} = 0 \qquad \text{for } \mathbf{x} \in \Omega_{env} \quad (7a)$$

$$-\nabla p + \nabla^2\mathbf{v} = 0, \quad \nabla\cdot\mathbf{v} = 0 \qquad \text{for } \mathbf{x} \in \Omega_{cyt} \quad (7b)$$

with the viscosity ratio defined by $\lambda = \mu_{env}/\mu_{cyt}$. These governing momentum conservation equations are subject to the following boundary conditions:

$\mathbf{v} = 0$, $|\mathbf{x}| \to \infty$
vanishing velocity (quiescence) at the infinity (8a)

$\mathbf{v} = 0$, $\mathbf{x} \in \partial\Omega_{elec}$
no slip condition on the electrode surface (8b)

$\mathbf{v} = \mathbf{v}_{mem}$, $\mathbf{x} \in \partial\Omega_{mem}$
no slip condition on the fused membrane (8c)

It should be emphasized that the scaling arguments indicate that the same Stokes system of equations is appropriate to describe the fluid motion in cases b and c, whereas case a does not require the fluid flow simulation.

Case (a): Serotonin Release by an Electroporated Granule of the Mast Cell. In the first case (case a) we consider the messenger diffusion in a freely suspended, electroporated granule matrix as the rate-controlling process for the microelectrode signal. This corresponds to the experimental studies performed by Marszalek

et al.[1,8] On the basis of the experimental conditions, the scales for the characteristic time, length, the messenger concentration, and fluid velocity are given by

$$t_{char} \sim t_{diff,matrix} \sim 3.1\ \text{s}, \quad l \sim R_0 \sim 2.5\ \mu\text{m} \tag{9}$$

$$C \sim C_0 \sim 3.37\ \text{mol/m}^3\ (3.37 \times 10^{-3}\ \text{M}), \quad \mathbf{v} \sim D_{matrix}/R_0 \sim 0.8\ \mu\text{m/s}$$

respectively. Here, C_0 is the initial concentration of serotonin in an isolated granule of the mast cell. In the experiments, electroporation was used to disrupt the granule membrane, and the pore expansion velocity was estimated to be close to 10 to ~25 μm/s.[8] With the use of the scaling arguments from the previous section, the serotonin concentration field in the extracellular fluid Ω_{env} is in a quasi-steady state, the advection mass transport is negligible in a quiescent fluid environment, and no homogeneous reactions involving serotonin take place. With these observations, the mass conservation equation, eq 5, governing serotonin transport in the extracellular fluid environment reduces to a simple Laplace equation

$$\nabla^2 C = 0, \quad \mathbf{x} \in \Omega_{env} \tag{10}$$

On the other hand, the serotonin transport inside of the granule matrix with fast swelling behavior is described by the transient diffusion−advection system with the local matrix bulk velocity **v** related to the matrix swelling deformation **u** ($\mathbf{v} = \partial\mathbf{u}/\partial t$)

$$\frac{\partial C}{\partial t} + \nabla\cdot(C\mathbf{v}) = D_{matrix}\nabla^2 C, \quad \mathbf{x} \in \Omega_{mat} \tag{11}$$

In eq 11, the bulk advection term $\nabla\cdot(C\mathbf{v})$ can be separated into a sum of two components, $\mathbf{v}\cdot\nabla C$ and $C(\nabla\cdot\partial\mathbf{u}/\partial t)$. Since we only consider small matrix deformation, we assume that the contribution from the first term is relatively small as compared to the divergence effect given by the second term $C(\nabla\cdot\partial\mathbf{u}/\partial t)$. Physically, the divergence term represents a pseudosink (dilution effect) in the system caused by the volumetric expansion of the granule. Since $t_{diff,matrix} > t_{diff,swell}$, the local matrix dilution effect dominates the system dynamics at the very beginning of the process and it vanishes as the process continues with the diffusion effect taking control at a longer time. The governing equation describing neurotransmitter transport in the granule matrix, eq 11, can be expressed in the following dimensionless form

$$\frac{\partial C}{\partial t} = \nabla^2 C - C(\nabla\cdot\partial\mathbf{u}/\partial t), \quad \mathbf{x} \in \Omega_{mat} \tag{12}$$

The system is completed by specifying the initial and boundary conditions, also expressed in a dimensionless form

$$C = 1,\ \mathbf{x} \in \Omega_{mat} \text{ at } t = t_0 \quad \text{uniform initial concentration} \tag{13a}$$

$$C = 0,\ \mathbf{x} \in \Omega_{env} \text{ at } t = t_0 \quad \text{vanishing initial concentration} \tag{13b}$$

$$C = 0\ |\mathbf{x}| \to \infty \quad \text{vanishing concentration at the infinity} \tag{13c}$$

$$C = 0,\ \mathbf{x} \in \partial\Omega_{elec} \quad \text{infinitely fast neurotransmitter oxidation} \tag{13d}$$

$$\partial C/\partial n = 0,\ \mathbf{x} \in \partial\Omega_{mem} \quad \text{nonpermeable membrane} \tag{13e}$$

$$C_{matrix} = C_{env},\ \text{x} \in \partial\Omega_{mat} \quad \text{continuity of the concentration field} \tag{13f}$$

$$D_r\nabla C_{matrix}\cdot\mathbf{n} = \nabla C_{env}\cdot\mathbf{n},\ \mathbf{x} \in \partial\Omega_{mat} \quad \text{continuity of the messenger flux through the matrix/solution interface} \tag{13g}$$

In the last eq (13g) the relative diffusivity is defined as $D_r = D_{matrix}/D_{bulk}$. The displacement of the swelling matrix and that of the matrix/solution interface is governed by the THB hydrogel model[17,18] described later as the second dynamic boundary condition. A constant lateral pore expansion speed is assigned to move the covering interface to mimic the pore opening effect. The coupling boundary conditions, eqs 13f and 13g, are applied to the interface where the pore is open, whereas eq 13e describes the rest of the interface as a nonpermeable membrane.

Case (b): Neurotransmitter Release by a Small and Clear Synaptic Vesicle. In the previous case, we focused on the serotonin transport in an electroporated granule of the mast cell with the temporal scale, $t_{diff,matrix}$, of the order of milliseconds. In case b, we change our focus to a much faster exocytotic event, that is neurotransmitter release by a small and clear (i.e., without a granule inside) synaptic vesicle.[5,13] The length/time scales for this process are in a nanometer/microsecond range and defined by the bulk diffusion in the extracellular fluid. The order-of-magnitude values for characteristic scales are given by

$$t_{char} \sim t_{diff,bulk} \sim 0.67\ \mu\text{s}, \quad l \sim R_0 \sim 20\ \text{nm} \tag{14}$$

$$C \sim C_0 \sim 270\ \text{mol/m}^3\ (0.27\ \text{M}), \quad \mathbf{v} \sim D_{bulk}/R_0 \sim 0.03\ \text{m/s}$$

Here, C_0 is the initial concentration of the neurotransmitter inside the clear vesicle at the beginning of the pore expansion process. On the basis of previous scaling results, the bulk advection effect can be neglected in describing the neurotransmitter transport in the extracellular fluid, owing to a very small Peclet number. Thus, a simple transient diffusion equation can be used to simulate

messenger transport

$$\frac{\partial C}{\partial t} = \nabla^2 C, \quad \mathbf{x} \in \Omega_{env} \tag{15}$$

with the initial and boundary conditions given by the following dimensionless forms:

$C = 1, \mathbf{x} \in \Omega_{vesicle}$ at $t = t_0$
uniform initial concentration (16a)

$C = 0, \mathbf{x} \in \Omega_{env} - \Omega_{vesicle}$ at $t = t_0$
vanishing initial concentration (16b)

$C = 0, |\mathbf{x}| \rightarrow \infty$ vanishing concentration at the infinity (16c)

$C = 0, \mathbf{x} \in \partial\Omega_{elec}$
infinitely fast neurotransmitter oxidation (16d)

$\partial C/\partial n = 0, \mathbf{x} \in \partial\Omega_{mem}$ nonpermeable membrane (16e)

In this case the vesicle is free of a granule matrix, and the lumen contained inside the vesicle, denoted by $\Omega_{vesicle}$, is considered to be a part of Ω_{env} with the constant diffusivity D_{bulk} assumed to be the same as in the solution environment.

Case (c): Adrenaline Release by a Medium Size Vesicle in the Chromaffin Cell. Case c includes the main aspects of the previous two models to simulate the release of adrenaline from the granule matrix enclosed by a vesicle of the chromaffin cell. We select $t_{diff,matrix}$ as the characteristic time scale to match the submillisecond temporal resolution of experiments reported in the literature.[10,11] On the basis of the experimental conditions, the reference values for the scaling parameters are given by

$$t_{char} \sim t_{diff,matrix} \sim 11.3\ \text{ms}, \quad l \sim R_0 \sim 150\ \text{nm} \tag{17}$$

$C \sim C_0 \sim 600\ \text{mol/m}^3$ (0.6 M),
$\text{v} \sim D_{matrix}/R_0 \sim 13.3\ \mu\text{m/s}$

where C_0 is the initial concentration of adrenaline inside the granule matrix. In the fluid domains, the quasi-steady diffusion−advection equation is applied

$$D_r(\mathbf{v}\cdot\nabla C) = \nabla^2 C, \quad \mathbf{x} \in \Omega_{env} \tag{18}$$

where the relative diffusivity is defined by $D_r = D_{matrix}/D_{bulk}$ as in case a. The neurotransmitter concentration within the granule matrix is described by the transient diffusion equations with the sink term on the right-hand side representing the matrix dilution due to fast swelling

$$\frac{\partial C}{\partial t} = \nabla^2 C - C(\nabla\cdot\partial\mathbf{u}/\partial t), \quad \mathbf{x} \in \Omega_{mat} \tag{19}$$

The initial and boundary conditions are given by

$C = 1, \mathbf{x} \in \Omega_{mat}$ at $t = t_0$ uniform initial concentration (20a)

$C = 0, \mathbf{x} \in \Omega_{env}$ at $t = t_0$ vanishing initial concentration (20b)

$C = 0, |\mathbf{x}| \rightarrow \infty$ vanishing concentration at the infinity (20c)

$C = 0, \mathbf{x} \in \partial\Omega_{elec}$
infinitely fast neurotransmitter oxidation (20d)

$\partial C/\partial n = 0, \mathbf{x} \in \partial\Omega_{mem}$ nonpermeable membrane (20e)

$C_{matrix} = C_{env}, \mathbf{x} \in \partial\Omega_{mat}$
continuity of the concentration field (20f)

$D_r\nabla C_{matrix}\cdot\mathbf{n} = \nabla C_{env}\cdot\mathbf{n}, \mathbf{x} \in \partial\Omega_{mat}$
continuity of the messenger flux through the matrix/solution interface (20g)

First Dynamic Boundary Condition: Large Deformation of the Fused Membrane. The first dynamic boundary condition describes the continuous expansion of the fusion pore and the unfolding behavior of the fused membrane, both modeled by a continuous deformation of a simple lipid bilayer structure. We assume that the large deformation of the membrane is driven by the local tension applied to the fused membrane and by the curvature-induced bending energy. We also assume that the simple fluid-like bilayer membrane has locally isotropic tension on the time scale of interest and has negligible shear elasticity. In our earlier works,[20,21] a generalization of the interfacial force jump condition for a two-fluid system has been developed by including the formalisms of the Helfrich's curvature energy theory[15,22] and Zhong-can's membrane mechanics.[16,23] To summarize these results, the surface force jump condition for the fluid interface is governed by a quasi-steady stress balance in the fluids[24] (cytosol and the extracellular environment in this case) adjacent to both sides of the membrane

$$(\boldsymbol{\tau}_{cyt}\cdot\mathbf{n} - \boldsymbol{\tau}_{env}\cdot\mathbf{n}) + \nabla_s\gamma - \gamma\mathbf{n}(\nabla_s\cdot\mathbf{n}) = 0, \quad \mathbf{x} \in \partial\Omega_{mem} \tag{21}$$

where $\boldsymbol{\tau}$ denotes the fluid stress tensor, $(\boldsymbol{\tau}_{cyt}\cdot\mathbf{n} - \boldsymbol{\tau}_{env}\cdot\mathbf{n})$ is the net surface traction induced by the hydrodynamic stresses from the adjacent fluids and acting along the surface normal $\mathbf{n}$. The fluid stresses are balanced by the isotropic local tension/compression of the membrane expressed in terms of $\nabla_s\gamma - \gamma\mathbf{n}(\nabla_s\cdot\mathbf{n})$, where ∇_s represents the surface gradient operator. The shear component $\nabla_s\gamma$ is given by the membrane tension gradient along the tangential direction $\mathbf{s}$ along the membrane surface, the normal component $\gamma\mathbf{n}(\nabla_s\cdot\mathbf{n})$ is defined by the membrane equilibrium shape equation.[16,23] Both terms solely depend on the instantaneous geometry of the evolving membrane and its elastic properties. An

(20) Fan, T.-H.; Fedorov, A. G. *Langmuir* **2003**, *19*, 10930−10939.
(21) Fan, T.-H.; Fedorov, A. G. *Langmuir* **2003**, *19*, 1347−1356.
(22) Deuling, H. J.; Helfrich, W. *Biophys. J.* **1976**, *16*, 861−868.
(23) Zhong-can, O.-Y. *Thin Solid Films* **2001**, *393*, 19−23.
(24) Scriven, L. E. *Chem. Eng. Sci.* **1960**, *12*, 98−108.

additional assumption of membrane local incompressibility, $\partial(dA)/\partial t = 0$, is enforced based on the membrane surface area constraint condition to complete the formulation since the local tension force γ is an additional unknown introduced by the boundary condition.[20,21] A general form of the constraint equation for a locally incompressible membrane was first derived by Pozrikidis[25] to study deformation of red blood cells in the shear flow, and it can be expressed in terms of the arc-length coordinate

$$\sigma\hat{\mathbf{t}}_s \frac{\partial \mathbf{v}}{\partial s} + \mathbf{v} \cdot \hat{\mathbf{e}}_\sigma = 0, \quad \mathbf{x} \in \partial\Omega_{mem} \tag{22}$$

where $\hat{\mathbf{t}}_s$ denotes the local surface tangent, σ is the coordinate along the radial direction, and $\mathbf{v}$ is the local migration velocity of the fused membrane.

Our simulations for case c calculate the membrane tension γ, which is an a priori unknown local parameter that drives the unfolding of the membrane, to be of the order of 10^{-6} N/m for higher membrane unfolding velocities. The compressibility modulus of various bilayer membranes reported in the literature[26] is of the order of 10^{-1} N/m. Clearly, for such a low area extension ratio the local incompressibility of the membrane[27,28] is a reasonable assumption that can be adopted for biological membranes. In principle, the Helfrich's curvature energy theory[15,16] is also applicable to describe an equilibrium state of a compressible membrane, although the membrane tension γ must now depend on the density of amphiphilic molecules within the two-dimensional fluid-like membrane and an additional conservation equation needs to be solved for the local density function.[29] Alternatively, for synthetic, not biologically native giant vesicles, it is possible to treat a stretchable membrane as a thin elastic sheet with an anisotropic elastic response along the principal directions, or consider the nonequilibrium phenomena by balancing the energy dissipation from the bulk fluid flow, the viscous motion of the membrane, and the time dependent line and surface energies.[30,31] The latter method is strictly applicable to the vesicle bilayers in a highly stretched state with nonfusion type pore dynamics and may not be appropriate for the fused membranes.

Second Dynamic Boundary Condition: Swelling Matrix Interface. Experimental results[1,8] suggest that the vesicle granule matrix increases by 30 to ~40% in radius and 2- to ~3-fold in volume during the swelling process as compared to its condensed state; thus, a dynamic boundary condition is required to describe the interfacial location of the swelling matrix. Further, the local internal elastic deformation of the matrix is needed to compute the pseudosink terms describing the matrix dilution effect in the messenger transport equations, eqs 12 and 19. To accomplish these objectives, we use the phenomenological THB hydrogel model[17,18] for an elastically expanding protein matrix. This theory is described by a simple differential equation, whose analytical solution can be explicitly integrated into our overall model describing the fluid flow membrane dynamics messenger transport. The origin of the THB model lies in the linear elasticity theory and incorporates an assumed Stokes-like friction force between the interlinked polymer network and the liquid solution during the swelling process. A brief derivation is given here starting from the general quasi-steady Cauchy equation of motion for a linear elastic body undergoing a small deformation

$$\nabla\cdot\boldsymbol{\tau}(\mathbf{x}) + \mathbf{F}(\mathbf{x}) = 0, \quad \mathbf{x} \in \Omega_{mat} \tag{23}$$

where $\mathbf{F}$ is the body force term, and τ_{ij} is the stress tensor for a linear elastic body. The constitutive relation between the stress and strain is linear and defined by the Hook's law

$$\tau_{ij} = K\frac{\partial u_k}{\partial x_k}\delta_{ij} + 2G\left(\frac{1}{2}\left(\frac{\partial u_i}{\partial x_j} + \frac{\partial u_j}{\partial x_i}\right) - \frac{1}{3}\frac{\partial u_k}{\partial x_k}\delta_{ij}\right) \tag{24}$$

where u_k is the equilibrium displacement vector, K is the bulk modulus of elasticity, G is the modulus of elasticity in shear, and δ_{ij} is the Kronecker delta function. In his pioneering paper,[17] Tanaka et al. postulated that a friction force in the polymer matrix should be simply added as a body force to Cauchy's equation. In this case, the interactions between the polymer network and the solvent contained in the matrix are represented by an effective friction coefficient f. By combining Tanaka's postulation $\mathbf{F} = -f\cdot(\partial\mathbf{u}/\partial t)$ and eq 24, the so-called "THB hydrogel model"[18] can be derived on the basis of eq 23:

$$\frac{\partial \mathbf{u}}{\partial t} = \frac{G}{f}\nabla^2\mathbf{u} + \frac{K + G/3}{f}\nabla(\nabla\cdot\mathbf{u}), \quad \mathbf{x} \in \Omega_{mat} \tag{25}$$

In the considered cases a and c, we assumed that the swelling of the protein matrix is uniformly triggered by the monovalent cations diffusing into the matrix from the extracellular solution. We further assume that the matrix is swelling uniformly and the spherical symmetry is maintained in the linear deformation process as observed in the spherical hydrogel system.[18] Then, for the cases a and c, wherein $t_{char} \sim t_{diff,martix}$, eq 25 can be reduced to the following dimensionless, spherically symmetric form

$$\frac{D_{matrix}}{D_{swell}}\left(\frac{\partial u_r}{\partial t}\right) = \frac{\partial}{\partial r}\left\{\frac{1}{r^2}\frac{\partial(r^2u_r)}{\partial r}\right\} \tag{26}$$

where u_r and r are the radial displacement and the spatial variable in the radial direction, respectively, and $D_{swell} = (K + 4G/3)/f$ represents an apparent collective diffusion coefficient determined by the elastic properties and the effective friction coefficient. In a typical case of $G \ll K$, the collective diffusion coefficient is approximated by $D_{swell} \sim K/f$ and is experimentally found to be ~1.4 $\times$ 10^{-11} m^2/s.[1] The eigenvalue problem for eq 26 was solved analytically[18] using an initial condition of the uniform, positive osmotic pressure π_0 that ensures the stress balance throughout the gel, $\sigma_{ij} = \pi_0\delta_{ij}$, the boundary conditions of central symmetry, $u(0,t) = 0$, and the stress-free outer interface of the gel, $\sigma_{rr} = 0$ at

(25) Pozrikidis, C. *J. Fluid Mech.* **1990**, *216*, 231−254.
(26) Marsh, D. *Biochim. Biophys. Acta* **1996**, *1286*, 183−223.
(27) Evan, E. A.; Skalak, R. *Mechanics and Thermodynamics of Biomembranes*; CRC Press: Boca Raton, FL, 1980.
(28) Seifert, U. Giant Vesicles: A Theoretical Perspective. In *Giant Vesicles*; Luisi, P.L., Walde, P., Eds.; Wiley: New York, 2000.
(29) Seki, K.; Komura, S. *Physica A* **1995**, *219*, 253−289.
(30) Brochard, F.; de Gennes, P. G.; Sandre, O. *Physica A* **2000**, *278*, 32−51.
(31) Sandre, O.; Moreaux, L.; Brochard, F. *Proc. Natl. Acad. Sci. U.S.A.* **1999**, *96*, 10591−10596.

$r = a$. The initial condition can be further reduced to equation, $K\nabla\cdot\mathbf{u} = \pi_0$, with the solution given by[18]

$$u_r(r,t_0) = \Delta a_0\left(\frac{r}{a}\right), \quad \Delta a_0 = \frac{\pi_0 a}{3K} \tag{27}$$

where π_0 is the initial uniform stress (positive osmotic pressure), a is final radius after swelling, Δa_0 is the total displacement of the interface, and $a - \Delta a_0$ is the initial radius of the matrix. The general solution of eq 26 is given by a series expansion in terms of eigenfunctions[18] for the radial displacement of the gel

$$u_r(r,t) = 6\Delta a_0 \sum_{n=1}^{\infty} \frac{(-1)^n}{n\pi}\left\{\frac{\cos(\beta_n r)}{\beta_n r} - \frac{\sin(\beta_n r)}{(\beta_n r)^2}\right\} \times \exp(-\hat{D}_r \beta_n{}^2 t), \quad r \in \Omega_{\text{mat}} \tag{28}$$

where $\beta_n = n\pi/a$ are the eigenvalues, $n = 1, 2, ..., \infty$, and the diffusivity ratio is defined by $\hat{D}_r = D_{\text{swell}}/D_{\text{matrix}}$. For reference, in both cases a and c considered in this work, the diffusivity ratio is around 7.0. Finally, it should be noted that the solution u_r represents the point displacement inside the network from its final equilibrium location after the matrix is fully swollen, that is, $u \rightarrow 0$ everywhere at $t \rightarrow \infty$. Accordingly, the divergence of the displacement velocity is

$$\nabla\cdot\frac{\partial \mathbf{u}(r,t)}{\partial t} = 6\Delta a_0 \sum_{n=1}^{\infty} \frac{(-1)^n}{n\pi}\left\{-\hat{D}_r \beta_n{}^2 \frac{\sin(\beta_n r)}{r}\right\} \times \exp(-\hat{D}_r \beta_n{}^2 t), \quad r \in \Omega_{\text{mat}} \tag{29}$$

The simplified THB model presumes that the swelling polymer matrix has a sharp interface separating the protein network from the surrounding liquid environment, and the radius of the moving interface is therefore given by $R_{\text{matrix}}(t) = a - u_r(a,t)$ with the diffusivity ratio assumed to be constant during the swelling process.

Faradaic Current Response. Once the messenger concentration field is determined everywhere, the Faradaic current response of the microelectrode can be obtained by integrating the local molecular flux over the active surface area of the electrode, including the conversion from dimensionless to dimensional form

$$I(t) = nFD_{\text{bulk}}C_0R_0\int_{\partial\Omega_{\text{elec}}} \nabla C\cdot\mathbf{n}\, \mathrm{d}A, \quad \mathbf{x} \in \partial\Omega_{\text{elec}} \tag{30}$$

where F is the Faraday constant, n is the valence number of the released neurotransmitter ($n = 4$ for cases a and b, and $n = 2$ for case c). Alternatively, the local current density distributed along the electrode surface can be computed as $i(t) = \mathrm{d}I(t)/(R_0{}^2\, \mathrm{d}A) = nFD_{\text{bulk}}C_0(\nabla C\cdot\mathbf{n})_{\partial\Omega_{\text{elec}}}/R_0$.

The intimately coupled governing equations for the fluid flow and neurotransmitter transport are reformulated in terms of integral equations based on the fundamental solutions of the Stokes[32,33] and Laplace differential operators. The coupled system of integral equations and dynamics boundary conditions are further reduced to an axisymmetric system by using the cylindrical coordinate transformation and expressing the fundamental solutions of the Stokes and Laplace operators in terms of the Green's functions of the ring-source type. The system is solved by the boundary integral method[33] and the dual reciprocity boundary element method.[34] Due to the limited space, the lengthy derivation of the integral equations and discretization method are not reported. The detailed model development and numerical implementation can be found in the reference;[35] thus, we only present the simulation results and compare them to the experimental data for the three case studies.

RESULTS AND DISCUSSION

Figure 2 presents the numerical results for the benchmark experiment a: an electroanalysis of serotonin transport in an electroporated granule of the mast cell. Although electroporation induces opening of the pores throughout the vesicle membrane, the simplest configuration with only two pores, located at the north and south poles of the vesicle, is simulated here. This simplification was suggested by Marszalek et al.,[1] and it is based on the observation that for large vesicles of the mast cell (radius about 2.5 μm) only the messengers released from the pore that is in an immediate vicinity to the microelectrode would contribute to the detected electrical current. At the very beginning, the current density is at its maximum at the center of the electrode as shown in Figure 2A. This corresponds to the shortest travel distance for the released serotonin to reach the electrode. The current peak magnitude increases in time, and the signal broadens due to an increase in the size of the pore opening with time. The normalized serotonin local concentration field shown in Figure 2B indicates that the concentration gradient is the greatest within the granule matrix near the interface, owing to almost 2 orders of magnitude smaller diffusivity in the granule matrix as compared to the bulk solution diffusivity. The resistance to the messenger transport near the interfacial region of the matrix is controlled by the open pore window size through which the messengers can leave the matrix, and this transient behavior is complicated by the increase of surface area and the volumetric diluting effects as the matrix swells. The characteristic rising time (~180 ms) and the magnitude of the total microelectrode current (~270 pA) in Figure 2C for the case of $V_0 = 25\mu$m/s are very consistent with the experimental results.[1,8] The current spike slowly decays until ~2000 ms when the entire serotonin content of the matrix is released to the environment.

In case b, the neurotransmitter transport by a small and clear synaptic vesicle is analyzed and shown in Figure 3. We used the pore size suggested by Stiles et al.[7] with the pore radius of 1 nm initially and increasing to 5 nm during the pore expansion. The

(32) Ladyzhenskaya, O. A. *The Mathematical Theory of Viscous Incompressible Flow*; Gordon & Breach: New York, 1969.
(33) Pozrikidis, C. *Boundary Integral and Singularity Methods for Linearized Viscous Flow*; Cambridge University Press: Cambridge, 1992.
(34) Partridge, P. W.; Brebbia, C. A.; Wrobel, L. C. *The Dual Reciprocity Boundary Element Method*; Computational Mechanics Publications: Southampton, 1992.
(35) Fan, T.-H. Fluid Mechanics and Bio-Transport Phenomena in Imaging of Biological Membranes Using AFM-Integrated Microelectrode. Ph.D. Dissertation, Georgia Institute of Technology, Atlanta, Georgia, 2003.

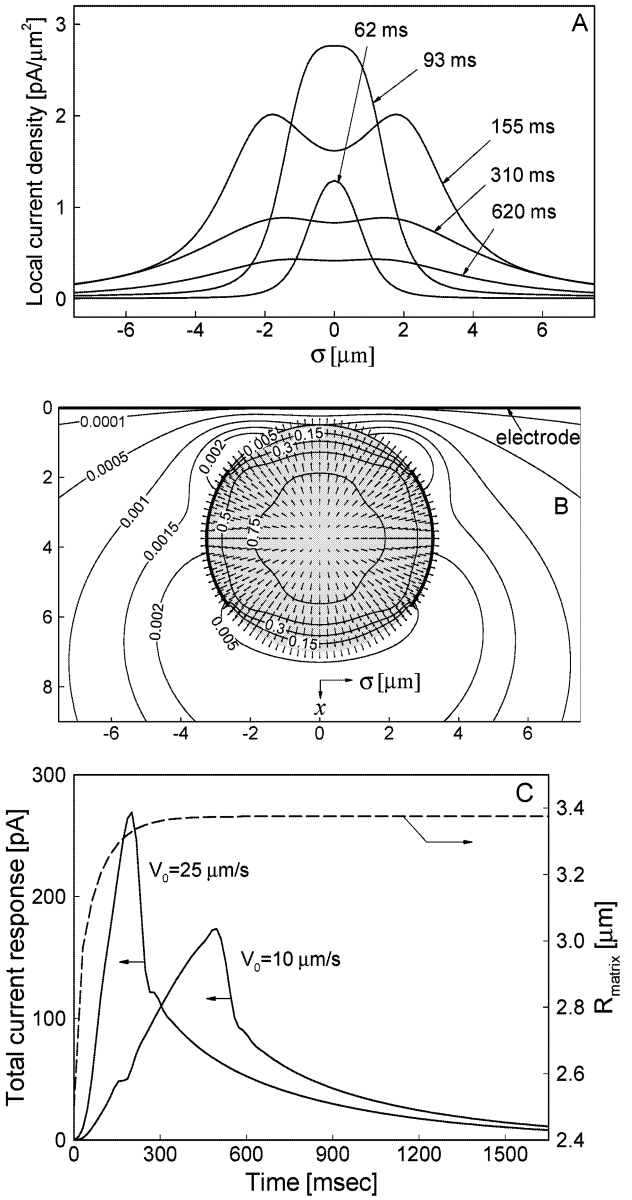

Figure 2. Simulation results for serotonin release by an electroporated granule: (A) transient, radially distributed local current density at the microelectrode for several consecutive time instances (pore expansion velocity V_0 = 25 μm/s is constant), (B) normalized instantaneous serotonin concentration field superimposed with the velocity field resulting from swelling of the granule matrix (time instant t = 155 ms and pore expansion velocity V_0 = 25 μm/s), (C) transient total current response (solid lines) for pore expansion velocities V_0 = 25 μm/s and V_0 = 10 μm/s, superimposed with the dynamics of the radius of the swelling matrix (dashed line) expanding from 2.5 to 3.375 μm.

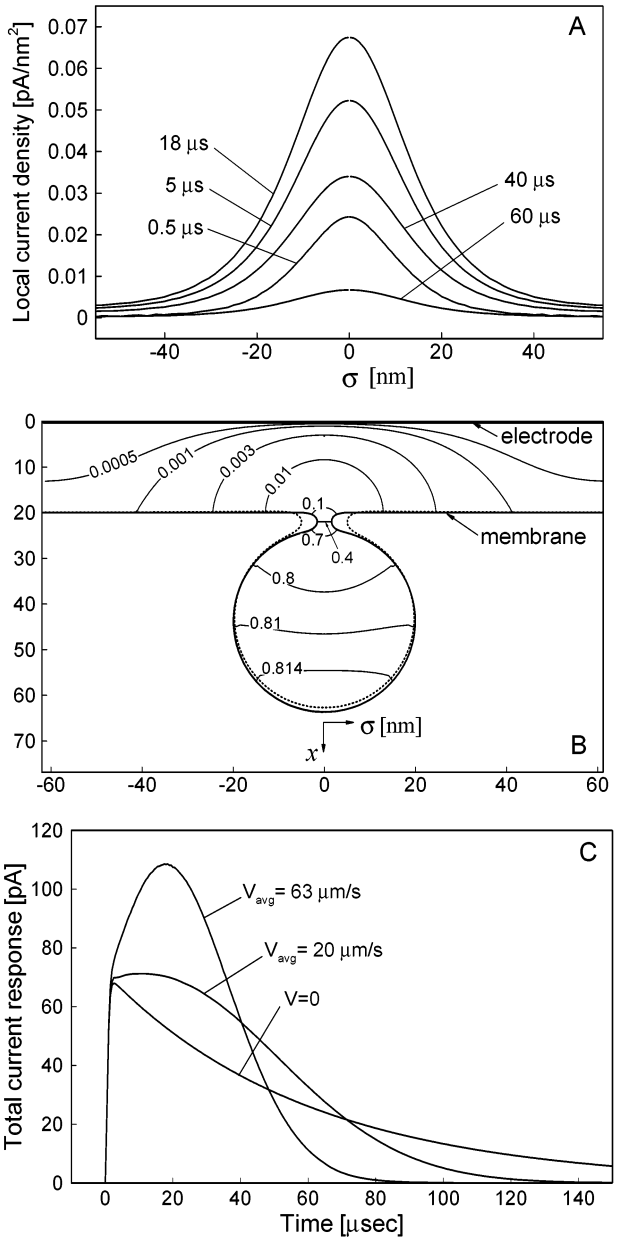

Figure 3. Simulation results of neurotransmitter release by a small and clear synaptic vesicle: (A) transient, radially distributed local current density at the microelectrode for several consecutive time instances (average pore expansion velocity ~63 μm/s), (B) normalized instantaneous serotonin concentration field (time instant t = 10 μs and an average pore expansion velocity ~63 μm/s), superimposed with the final membrane position (dotted line) with the pore opening radius of 5 nm, (C) transient total current response for the average pore expansion velocities V_{avg} = 63, 20, and 0 μm/s.

magnitude of the current density, shown in Figure 3A, is always maximum at the center of the electrode, which corresponds to the shortest diffusion path through the pore for the released neurotransmitter to reach the electrode. There is no granule matrix in the small and clear synaptic vesicle, and the normalized concentration field shown in Figure 3B indicates the greatest concentration gradient within the neck area of the narrow fusion pore, implying that this is the area of the bottleneck resistance to the molecular transport. The total current response curve measured in the typical exocytosis experiments[6] using microelectrode is demonstrated in Figure 3C for three representative pore expansion velocities of 0, 20, and 63 μm/s. The model predicts a spike shape which is similar to the experimental results[6] with an instantly rising phase and a longer decaying tail. However, the rise time to the maximum total current response, computed to be less than 18 μs, is overpredicted as compared to the reported experimental values of 25 to ~80 μs[7] and ~90 μs[6] for the neurotransmitter release from the small synaptic vesicles. Further, our predictions indicate that the current spike can reach a value greater than 100 pA, which is more than an order-of-magnitude higher than the experimental result, ~5 pA, measured by Bruns

and Jahn.[6] The significant difference between predictions and experiments in both the amplitude and time constant may be caused by the diffusion broadening effect due to an uncertain positioning of the microelectrode, a reduction in the number of messengers released due to the "kiss and run" events,[10] or a smaller diffusivity of the lumen region inside the small vesicle as compared to the bulk extracellular environment value that we assigned to it in our simulations. Although the model may discount some important phenomena leading to lack of quantitative agreement, there appears to be an equally valid need for a carefully controlled experiment to establish the true picture of the actual phenomena.

In case c, we simulate adrenaline release by a medium size vesicle in chromaffin cells. The biophysical parameters from the simultaneous amperometry and membrane capacitance measurements by Amatore et al.[11] are used as an input in our simulations. A two-stage process was conceptually suggested by amperometric experiments showing a constant rate of the neurotransmitter release (the current plateau) through a stable fusion pore (the "pore-release" stage with the low pore expansion velocity) followed by a sudden increase in current through an enlarged pore with the granule matrix totally exposed to the extracellular environment (the "full-fusion" stage with the high pore expansion velocity).[11] Our model interprets the experiments by including several key features that are absent in the semiempirical model:[10] (i) We account for the fact that a granule matrix is surrounded by the lumen fluid before and after the small fusion pore is opened as well as during the swelling process. We do not impose the constraint on the matrix interfacial area exposed to the fluid medium but allow it to expand according to the THB swelling model. Similar molecular diffusivities are assumed for the monovalent ions in both lumen and extracellular fluids that trigger the matrix swelling. Thus, local electroneutrality is maintained owing to an immediate replenishment of counterions that surround the granule matrix during the swelling process. (ii) Both the membrane dynamics and messenger transport are simultaneously considered with a minimum number of physically meaningful tuning parameters to match the experimental results. (iii) The pore edge energy is not considered in our model. Instead, the surface energy is indirectly evaluated from the computed local tension force γ rather than approximating the nonequilibrium pore energy using equilibrium thermodynamics.[10] The magnitude of the tension force far away from the pore is assigned to match the apparent pore opening velocity measured in experiments. (iv) The advection effect induced by the suddenly enlarged pore promotes and locally redistributes the molecular flux to the electrode surface and is accounted for. It is demonstrated that the advection contribution is significant, especially for the cases with higher Peclet number flows corresponding to the vesicles whose size is comparable to or greater than the nominal size ($R_0 \geq 150$ nm) of vesicles in chromaffin cells and for a higher pore opening velocity ($V_0 \geq 18$ μm/s).

In Figure 4A, the local current density detected by a microelectrode increases slowly during the initial "pore-release". After a predefined time of 10 ms, the fast "full-fusion" stage starts and the current density instantly rises to its maximum value around 3300 pA/μm^2, with a rise time of only 2 ms, and then slowly decays with the time to full decay about 8 ms. A drastic change in the

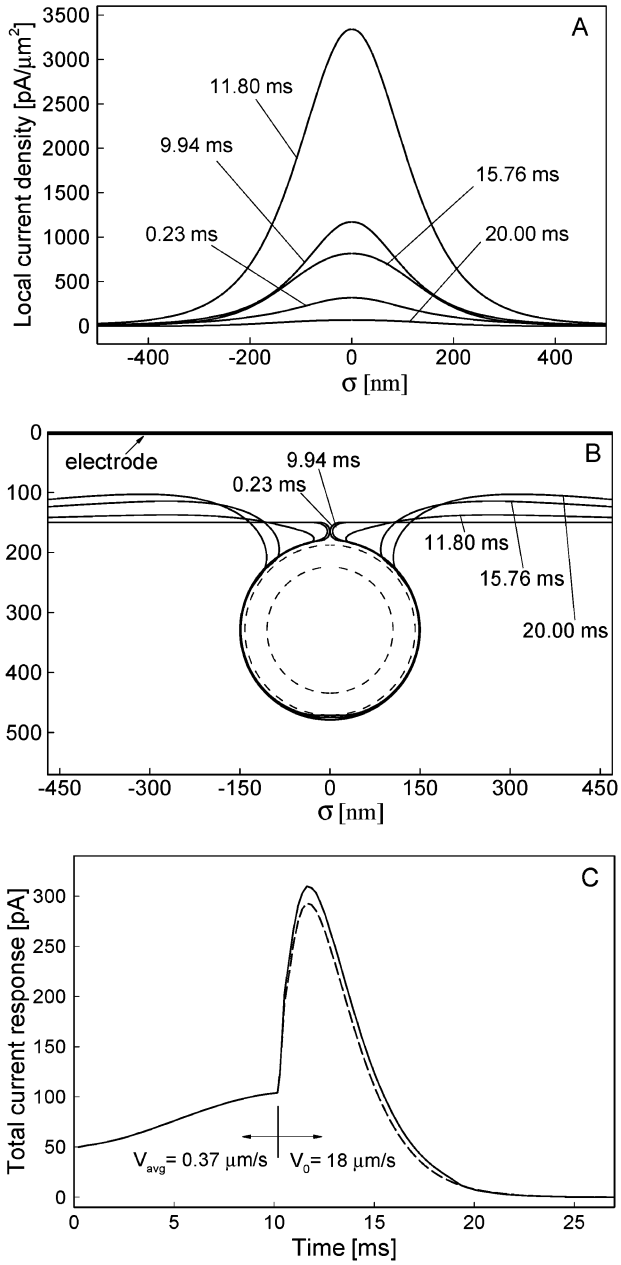

Figure 4. Simulation results of adrenaline release by a medium size vesicle in a chromaffin cell: (A) transient, radially distributed local current density at the microelectrode for several consecutive time instances, $t = 0.23$, 9.94, 11.80, 15.76, and 20.00 ms, (B) instantaneous snapshots of the dynamic membrane evolution corresponding to the time instances of the plot in A, superimposed with the initial and final interfacial locations (dashed lines) of the granule matrix, (C) transient total current response in the two-stage pore opening process (a slow "pore-release" at 0.37 μm/s and a fast "full-fusion" at 18 μm/s), superimposed with the case (dashed line) simulated where the fluid advection effect is neglected.

messenger flux (as expressed by the total microelectrode current) for the slow-to-fast stage transition is also well illustrated by Figure 4C, where the signal slowly increases from 50 to 120 pA during the "pore-release" stage followed by an almost immediate current spike to a peak value of up to 310 pA in the beginning of the "full-fusion" stage. The simulated shape of the current spike and its decay, as shown in Figure 4C, agree very well with the experimental results.[10,11] However, there is quantitative disagreement

between our predictions using the medium vesicle size ($R_0 = 150$ nm) and the experimental data:[10,11] The predicted magnitude of the current spike is four to five times higher, i.e., predicted 310 pA versus measured 60 to ~80 pA, and the decay is three to four times faster, i.e., predicted 10 ms versus measured 30 to ~40 ms. This significant difference between predictions and experiments in both the amplitude and the time constant could be due to finite electrode kinetics, a greater diffusion resistance in the lumen fluid between the granule matrix and the vesicle membrane, the nonhomogeneous diffusivity inside the granule matrix caused by partially exposed matrix interface and highly localized swelling dynamics, or a very complex interaction induced by an extrusion behavior of the granule matrix. The inclusion of advective transport associated with the bulk extracellular fluid motion enhances the amplitude of the current spike by 5 to ~6% for a pore opening velocity of 18 μm/s, as shown by comparison with the simulation with neglected advection (dashed line) in Figure 4C.

CONCLUSIONS

We have developed an integrated theoretical model to simulate the biotransport phenomena underlying dynamics of exocytotic events for several different vesicle/cell types with application to electroanalysis. The model considers the opening and expansion of the fusion pore, vesicular matrix swelling, elastic membrane unfolding, and molecular messenger release in the limits of the continuous fluid transport and elasticity theories. The theoretical results are compared with the experiments, and in general, a very good qualitative agreement is found between simulations and experiments. Analysis of the model predictions provides basic understanding of the slow and fast steps in an exocytotic sequence, thereby allowing for verification of competing hypotheses on what controls/limits the messenger release during exocytosis. Further improvement of the model to reach quantitative agreement demands a more detailed experimental and theoretical work to refine the biophysical fundamentals beyond the current state of understanding.

ACKNOWLEDGMENT

This research was supported by NIH Grant RO1 EB000508-01A1 and NSF Grant CE-BIO-0216368.

Received for review February 13, 2004. Accepted May 21, 2004.

AC049748G